멤브레인(Membrane Journal)
Vol.12, No.2, June, 2002, 97-106

스피노달 분해와 기핵성장에 따른 상분리 과정의 광산란 패턴의 관찰

강 종 석[1] · 허　훈 · 이 영 무[†]

서울 성동구 행당동 한양대학교 공과대학 응용화학공학부
(2002년 5월 24일 접수, 2002년 6월 14일 채택)

The Observation of Scattering Patterns During Membrane Formation: Spinodal Decomposition and Nucleation Growth

Jong Seok Kang[1], Hoon Huh, and Young Moo Lee[†]

National Research Laboratory for Membrane, School of Chemical Engineering,
College of Engineering, Hanyang University, Seoul 133-791, Korea
(Received May 24, Accepted June 14, 2002)

요　약 : Polysulfone (PSf)/NMP/alcohol 용액과 chlorinated poly(vinyl chloride) (CPVC)/THF/Alcohol 용액에 대한 광산란 패턴을 SALS (Small angle light scattering)와 FE-SEM (field emission scanning electron microscope)을 이용하여 조사하였다. PSf 용액에서는 시간에 따라 q값의 최대 산란 강도를 보이는 광산란 거동을 나타내어 스피노달 (SD) 상분리 거동을 나타내는 반면, CPVC 용액에서는 q값이 증가함에 따라 광산란 강도가 줄어드는 핵성장 (NG) 거동을 나타냈다. 각 고분자 용액에서 상분리 중반과 후반부에서 비용매 첨가제로 사용된 알코올의 탄소수가 증가할수록 농도분극의 증가율은 줄어들었다. 또한, SD에서의 초반부의 시간에 따른 산란 강도는 비용매 첨가제의 종류에 무관하게 Cahn의 선형 이론에 잘 부합되었다. 또한, SALS 장치로 얻어진 기공크기와 전자현미경으로 얻어진 영역 크기는 상호간에 비교되었다. 20PSf/70NMP/10n-butanol (w/w%) 용액에 대한 산란 패턴은 초기 상분리 거동에서부터 후기 거동까지 매우 선명하게 관측되었고, 초반, 중반, 그리고 후반부에 대한 SD에 대한 이론적 결과와 잘 일치하였다. 최고의 산란강도를 나타낸 각도의 크기는 n-butanol > n-propanol > methanol > no alcohol 순으로 관찰되었으며, 이 순서로 최종 형성된 막 단면의 기공 크기가 감소되는 것으로 조사되었다.

Abstract : Small angle light scattering (SALS) and field emission scanning electron microscope (FE-SEM) have been used to investigate the light scattering patterns with time evolved during water vapor quenching (relative humidity of 53 (±3)% at 26°C) of polysulfone (PSf)/NMP/Alcohol and chlorinated poly(vinyl chloride) (CPVC)/THF/Alcohol, respectively. Time dependence of the position of the light scattering maximum was observed at PSf dope solutions, confirming spinodal decomposition (SD), while CPVC dope solutions showed a decreased scattered light intensity with an increased q-value, indicating nucleation & growth (NG). For the each system, domain growth rate in the intermediate and late stage of phase separation decreased with increasing the number of carbon of alcohol used as additive (non-solvent). Also, in the early stage for SD, the scattering intensity with time was in accordance with Cahn's linear theory of spinodal decomposition, regardless of types of non-solvent additive. Also, the size scales obtained by SALS were mutually compared to domain sizes gained by FE-SEM measurement. These observations of scattering pattern were much clearly observed for the 20PSf/70NMP/10n-butanol (w/w%)

[†]주저자(e-mail : ymlee@hanyang.ac.kr)
본 논문은 2002년 춘계 학술발표논문상 수상논문임.

and agreed with the theoretical predictions for scattering patterns of each stage like the early, the intermediate, and the late stage of SD type phase separation. As the scattering maximum was observed at the larger angles (larger q) in the order of n-butanol > n-propanol > methanol > no alcohol, the pore size of final morphology decreased.

Keywords : *water vapor induced phase separation, polysulfone, chlorinated poly(vinyl chloride), small angle light scattering (SALS), pore size.*

1. Introduction

Microfiltration, which covers the pore size ranging between 0.1 and 10 μm, has been widely used to separate liquid/liquid or liquid/solid mixtures. Different membrane separation processes require different membrane structures to bring about good separation performance. Also, separation property of microporous membranes is mainly determined by the pore diameter in membrane surface as well as surface chemical properties. Therefore, it is important to fabricate membranes with pore size suitable for the specific application. Porous polymeric structures are mainly prepared by the controlled phase separation of polymer solutions[1]. Phase separation of polymeric solutions can be induced in several ways: nonsolvent-induced phase separation (NIPS), thermally induced phase separation (TIPS), and pressure-induced phase separation (PIPS). For air casting (dry casting) of a polymer solution, precipitation from the vapor phase, and immersion precipitation are typical processes for the nonsolvent-induced phase separation[2]. Considering that the activity of water in a vapor phase is similar to that in a liquid phase, phase inversion process by the water vapor induced phase separation might be a similar mechanism with that by liquid water because the thermodynamic state of all the other components are the same. Therefore, the difference in two cases seems not to be originated from the differences of thermodynamic terms, but from the differences of kinetic terms.

The separation of homogeneous mixture into two phases can proceed through two main ways, spinodal decomposition (SD) and nucleation growth (NG) [3,4] The selection of the mechanism depends on the thermodynamic balance between the two components and is mainly driven by the quenching depth and the composition. SD takes place if the mixture is quenched into an unstable region of the phase diagram. The growth of domain originates from a small and periodic fluctuation of composition, indicating the transformation from a homogeneous mixture with a single refractive index to a mixture with two distinct phases (thus with two different refractive indexes). The mean distance between the regions and the increase of concentration of the major component in their respected phases are well documented[5]. When the process occurs between binodal and spinodal (metastable region), this process is called "nucleation and growth (NG)." The solution is stable to small fluctuations but undergoes phase separation for large concentration fluctuations. A dispersed phase consisting of droplets of a polymer poor solution is formed in a concentrated matrix. The composition inside the nuclei would be not change with time, and only the size of the droplets increases with time. The molecules that feed the new phase follow ordinary transport phenomena by downhill diffusion with a positive diffusion coefficient.

The observation of the angular distribution of scattered light pattern made it possible to establish the phase separation mechanism of NG or SD. In both cases, since the system will be transformed from a homogeneous mixture with singe refractive index to a mixture with two different refractive indexes, small angle light scattering (SALS) is the obvious and the most simple tool to study such phase separation in the type of systems under consideration here[6-9]. The availability of SALS depends on the length scale window of interest. In this paper, SALS technique widely used for the investigation of phase separation mechanism was applied to confirm the phase separation mechanism for CPVC/THF/alcohol and PSf/NMP/Alcohol, respectively.

This paper presents full scattering patterns of SD

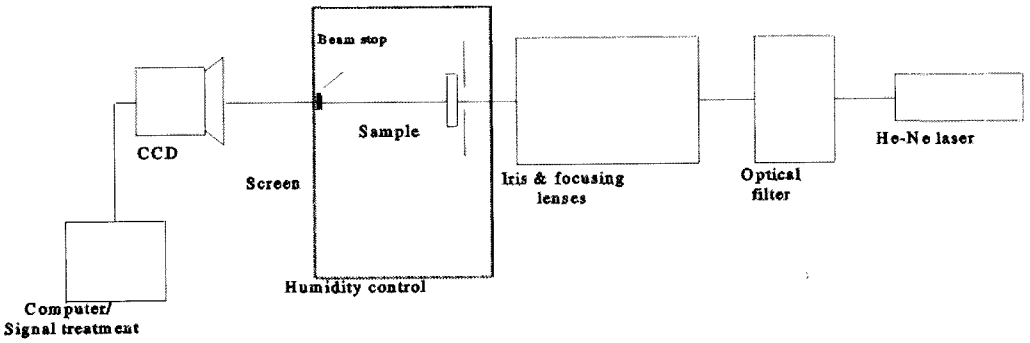

Fig. 1. Schematic of small angle light scattering apparatus.

from early stage to intermediate & late stage for PSf dope solutions and the role of alcohol additive like methanol, ethanol, n-propanol, and n-butanol on scattering patterns. Also, the phase separation of CPVC/THF/alcohol system was followed by characteristic scattering patterns of NG.

2. Experimental

2.1. Materials and Dope solutions:

A polysulfone (PSf, BP Amoco Chemicals, Udel-P3500, GA, U.S.A.) and chlorinated poly(vinyl chloride) (CPVC, Nippon Carbide Ind. Co. Inc., Tokyo, Japan) with a chlorine content of about 63-68% were used as a base material. 1-methyl 2-pyrrolidone (NMP), tetrahydrofuran (THF) (Aldrich Chemical Co., Milwaukee, WI, U.S.A.), and alcohols like methanol, ethanol, n-propanol, and n-butanol (Junsei Co., Tokyo, Japan) were used as solvent and nonsolvent additives, respectively. These reagents were used as received without further purification. PSf was washed with methanol and then dried under vacuum at 50°C for at least 4hrs in order to extract the residual methanol in the polymer prior to the preparation of the solution. The dope solutions were composed of 20PSf/70NMP/10alcohol (w/w%) and 9CPVC/61THF/30alcohol (w/w%), respectively. Polymer dope solutions were prepared by altering the kind of alcohol, i.e., increasing the number of carbon of alcohol.

2.2 SALS and FE-SEM measurements

The setup of small angle light scattering (SALS) apparatus was described in detail elsewhere[10] and only a brief account was given here. The scattering intensity, I, is measured as a function of the magnitude, q, of the scattering vector, denoted by $q = [4 \sin(\theta/2)]/\lambda]$ where q is the magnitude of the scattering vector, is the scattering angle of the intensity maximum, and λ is the wavelength of the light (He-Ne 632.8 nm, 10 mW), respectively. As shown in Fig. 1, a collimated laser beam impinges into sample, which is located in the rectangular glass chamber (30 $\times$30$\times$25 cm) connected with the humidity controller (JEIO Tech. Model Sk-G001, Seoul, Korea). Both the transmitted and scattered light were projected on the opaque screen at the upper side of the rectangular glass chamber in whose focal plane a beam stop blocks the directly incident beam and the images of scattered light were recorded and digitized by the CCD (NTC/CCD-512-TK, Roper Scientific™, Trenton, NJ, U.S.A.) with ST-133 controller. This setup allowed us to measure $I(q)$ over scattering vectors in the range of $0.398\ \mu m^{-1} < q < 3.72\ \mu m^{-1}$, corresponding to angles from 2.3° to 21.6°.

The morphologies of the quenched films after SALS experiment were also determined using field emission scanning electron microscope (FE-SEM, JEOL-6340F, Kyoto, Japan) at an accelerating voltage of 15kV. Scattering cell was immersed in water to extract the residual solvent (NMP/alcohol or THF/alcohol) and to solidify the resultant structure of film and then dried in vacuum at 30°C for 1 day. Dried specimen was fractured under cryogenic condition using liquid nitrogen and coated with gold, for taking the FE-SEM photographs.

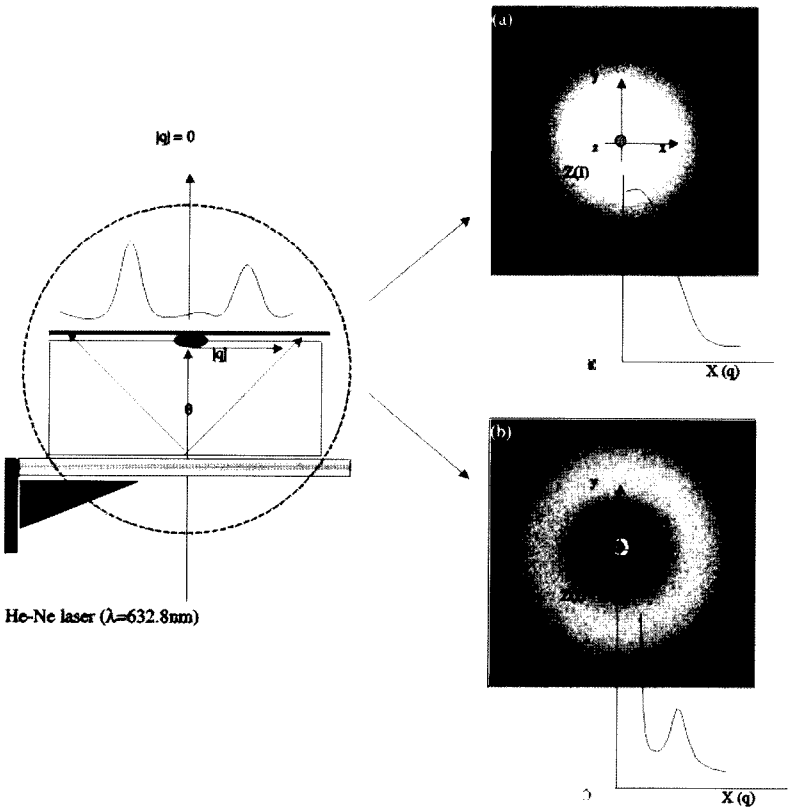

Fig. 2. Typical scattering patterns of phase separation processes: (a) nucleation & growth, (b) spinodal decomposition.

3. Results and Discussion

3.1. Scattering during Liquid-Liquid Phase Separation

As far as liquid-liquid demixing of polymer solution is considered, two different mechanisms have to be considered: nucleation growth (NG) and spinodal decomposition (SD). NG is the expected mechanism when a system leaves the thermodynamically stable condition and slowly enters the metastable region of phase diagram, between the bimodal and the spinodal line. Dispersed nuclei are formed and become stable if the activation energy for nucei formation is higher than the surface free energy. NG is usually a slow process, and a large number of polymeric systems have been reported in the literature in which phase separation follows the NG[11,12]. For the investigation of NG, time resolvable light scattering measurements with angle dependence have been especially useful. As illustrated in Fig. 2, when the NG mechanism predominates, a monotonic decrease of scattered light intensity with angle is normally observed[13]. At a fixed angle, the increase of scattered light intensity can be fitted to a power law[14]. However, in case of phase separation accompanied by any chemical reaction, these power law equations are not considered.

Meanwhile, a large number of polymeric systems have been reported in the literature in which phase separation follows the spinodal decomposition[10,17]. For the investigation of SD, time resolvable light scattering measurements with angle dependence have been especially useful. As shown in Fig. 2, light passing through the SD structure with high periodicity is diffracted, forming a scattering halo. The halo formation can be better understood in the following way. During spinodal decomposition, each concentration fluctuation with a wavenumber q, indicating the correlation length in a network of entangled polymers (or the size of aggregates in solution), contributes to

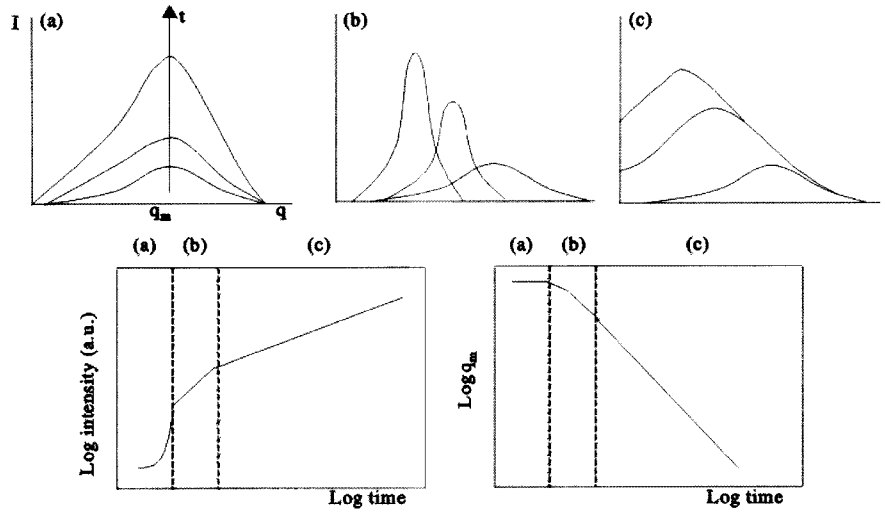

Fig. 3. Schematic drawing of the evolution of the scattering peak during spinodal decomposition. Data was taken from ref. 17.

diffraction at an angle θ.

In early stage described by the Cahn-Hilliard linearised theory[16], some fluctuations with a wavenumber q_m were predominant and contributes to a maximum scattered light intensity at an angle θ_m, giving rise to the observed halo. Also, the evolution of the structure factor with time was characterized by an exponential growth with a fixed maximum located around q_m.

It was reported that general expressions of the evolution of the structure factor, taking into account the non-linearities contained in the diffusion equation [17]. In the intermediate stage of SD, an evolution of the scattered peak to the small wavevectors, corresponding to the growth of the domains. As the concentration fluctuations grow, the amplitude of the fluctuations grows. At the moment the equilibrium concentrations in each phase are reached, the system enters the final stage. In the final stage of SD, the self-similar growth of the morphology is observed. Generally, the intermediate and late stages of spinodal decomposition are often described in terms of power law relationships proposed by Liu and Kiran[18]. The evolution of the structure factor during SD with time was summarized in Fig. 3. Note that the light intensity increased with time around beam stop ($q<q_m$), as indicating the late stage of SD. Therefore, the discrimination between early stage and late stage of SD was clearly confirmed from the scattering patterns with time evolution.

3.2. The Observation of Time-Resolved Light Scattering Patterns during NG

The evolution of light scattering patterns with time during quenching to water vapor of RH53% were observed for CPVC solutions (CPVC/THF/ROH = 9/61/30 wt%), where the alcohols like ethanol, n-propanol, and n-butanol were used as the nonsolvent additive within dope solution, respectively. All scattering pictures were presented as detected by the CCD camera without subtracting a background image, where the time indicated presented the elapsed time of each experiment. The run was sufficiently lasted for the several minutes in order to observe the full stage behavior of NG as clear as possible. The existence of the fractal regime at very small scattering vectors ($q \ll R^{-1}$) reveals the existence of structures on length scales larger than R, where R is the size of the supermolecular structure; this can result from the presence of large aggregates or from entanglements in concentrated solutions. The fractal dimension at low q provides a measure of the supramolecular organization of the solution. In these cases, a concentration

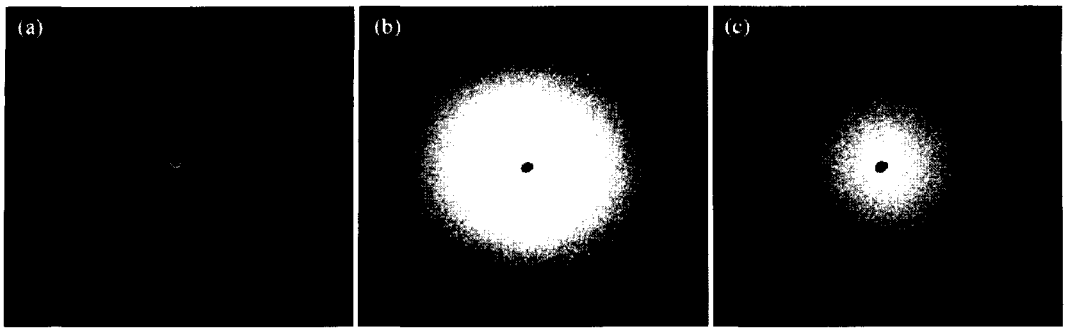

Fig. 4. Representative SALS patterns for proceeding phase separation of 9wt% CPVC solution/ 61wt% TFH/30wt% n-butanol system under RH53% (±3%) at 26°C (a) 117.0 sec, (b) 271.5 sec, and (c) 294.0 sec.

fluctuation of polymer solution may be visible at low q, indicating the correlation length (in a network of entangled polymers), or the size of aggregates in solution. As already described in experimental section, This setup allowed us to measure $I(q)$ over scattering vectors in the range of 0.398 $\mu m^{-1} < q < 3.72$ μm^{-1}, showing the fluctuation of the supramolecular organization of the solution within the several microns scale.

Representative light scattering patterns were shown in Fig. 4. It was seen from Fig. 4 that after ca. 120 sec from water vapor exposure the corn-typed scattering pattern appeared in the detectable region; immediately the maximum intensity increased and became broader with time. Thereafter, as indicated the late stage of the phase separation process, a scattering intensity finally became weak and decreased with time, as maintained a smaller corn-typed pattern. These characteristic SALS patterns showed a typical phase separation according to NG. It could be observed from Fig. 4 that the scattering maximum appeared within experimental time scale; immediately the maximum intensity increased and became broader with time. Thereafter, as indicated the late stage of the phase separation process for SD, a scattering intensity inner side of halo distinctively appeared during very short time-interval and finally got closer to the first and then turned into a broader one of corn-typed pattern. Therefore, the discrimination of scattering pattern at the late stage of SD and NG was not clearly observed due to a similar SALS patterns. It could be considered that phase separation was interrupted by gelation, glass transition, or crystallization[15]. In early stage of phase separation, it could be relatively well distinguish between NG and SD from SALS pattern.

3.3. The Observation of Light Scattering Patterns with time evolution during a SD

Figs. 5~8 show the evolution of light scattering patterns during quenching to water vapor of RH53% for transparent Psf solutions (Psf/NMP = 20/80 wt%, Psf/NMP/ROH = 20/70/10 wt%), where the alcohols like methanol, n-propanol, and n-butanol were used as the nonsolvent additive within dope solution, respectively. The run was sufficiently lasted for the several minutes in order to observe the full stage behavior of SD as clear as possible. To our knowledge, the practical observation of the full scattering patterns with time evolution was firstly reported within a reasonable time scale due to the slow preceding rate of phase separation by using the nonsolvent (water) of vapor state. It was seen from Fig. 5 that after ca. 109 sec from water vapor exposure the scattering maximum appeared in the detectable region; immediately the maximum intensity increased and became broader with time. Thereafter, as indicated the late stage of the phase separation process, a scattering intensity inner side of halo distinctively appeared during very short time-interval (indicated as the arrow in the Figs) and finally got closer to the first and then turned into a broader one of corn-typed pattern. Also, from Figs. 6~8, an intense halo-typed scattering pattern appeared after 114sec (methanol), 267 sec (n-propanol), and 292 sec (n-butanol), respectively. Then the characteristic scattering patterns of late stage as stated above

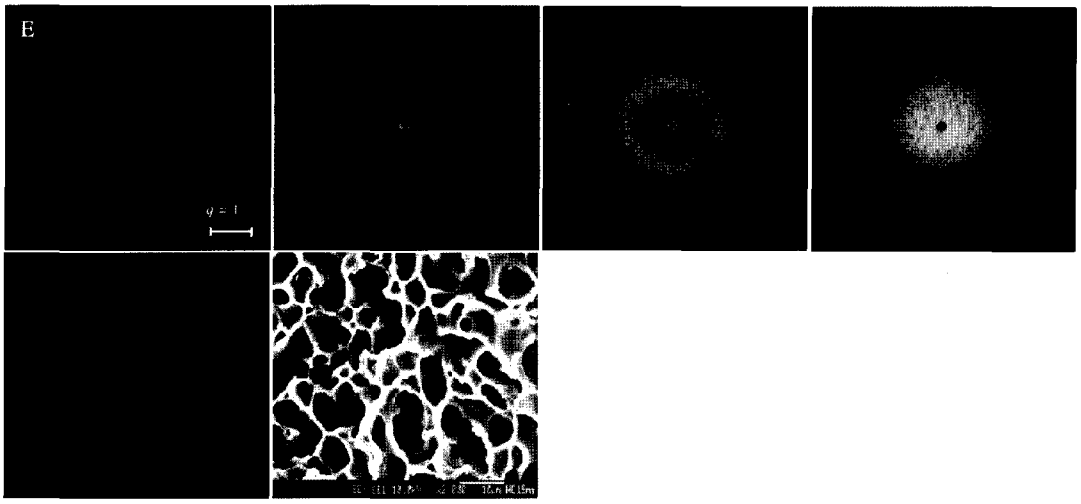

Fig. 5. The light scattering pattern progressed as a function of time during phase inversion process under water vapor of RH53% using 20Psf/ 80NMP (w/w%). FE-SEM photographs at the right bottom taken from specimen after SALS experiment show the final cross-sectional morphology. E, I, and L show the early stage, intermediate stage, and late stage, respectively. This notation and FE-SEM was equally applied to Fig. 6, 7, and 8.

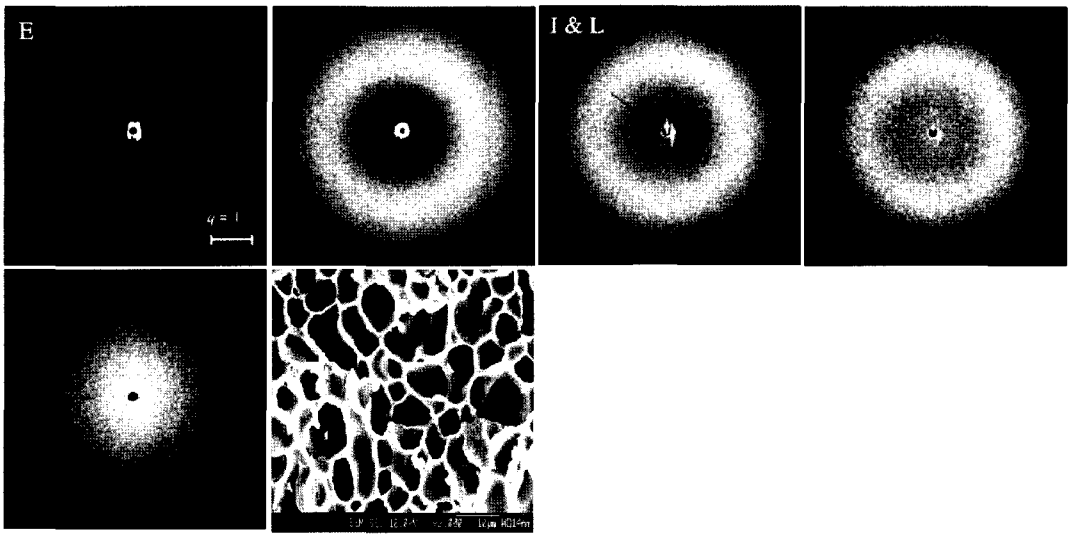

Fig. 6. The scattered light pattern progressed as a function of time during SD for 20Psf/70NMP/ 10methanol (w/w%).

showed for a long time-scale. Therefore, the presence of a maximum intensity and its progressive shift to lower wavenumbers were characteristics of phase separation by spinodal decomposition[16-20]. In the late stage of the phase separation process, this corn-typed pattern could be clearly seen in Fig. 5~8. It was noticeable that in case of the scattering of dope solution containing methanol or n-propanol the intermediate and late stage of SD was predominantly observed, while in the case of n-butanol the overall scattering patterns progressed between the early and the late stage of phase separation by SD were clearly

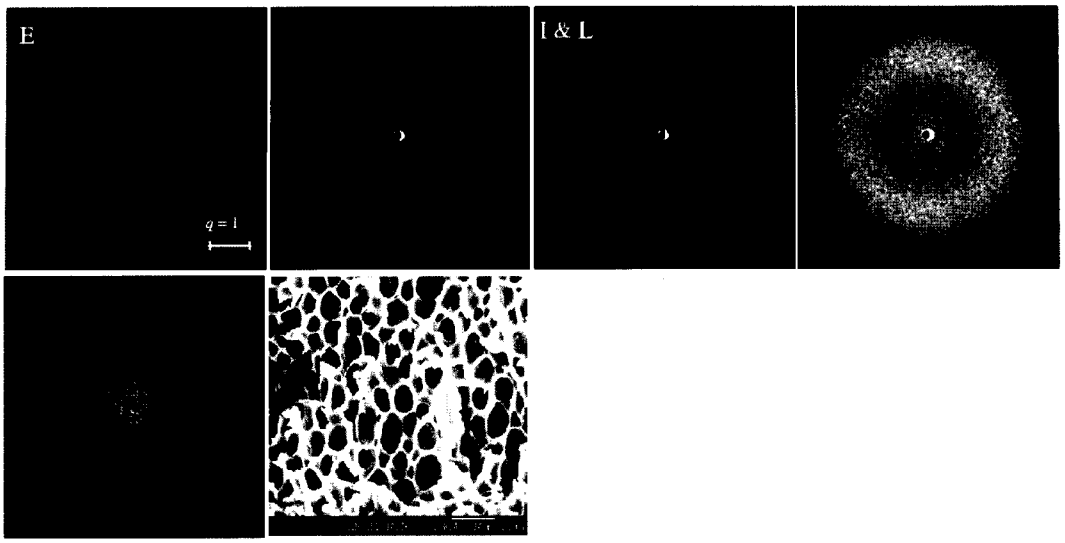

Fig. 7. The scattered light pattern progressed as a function of time during SD for 20Psf/80NMP/ 10n-propanol (w/w%).

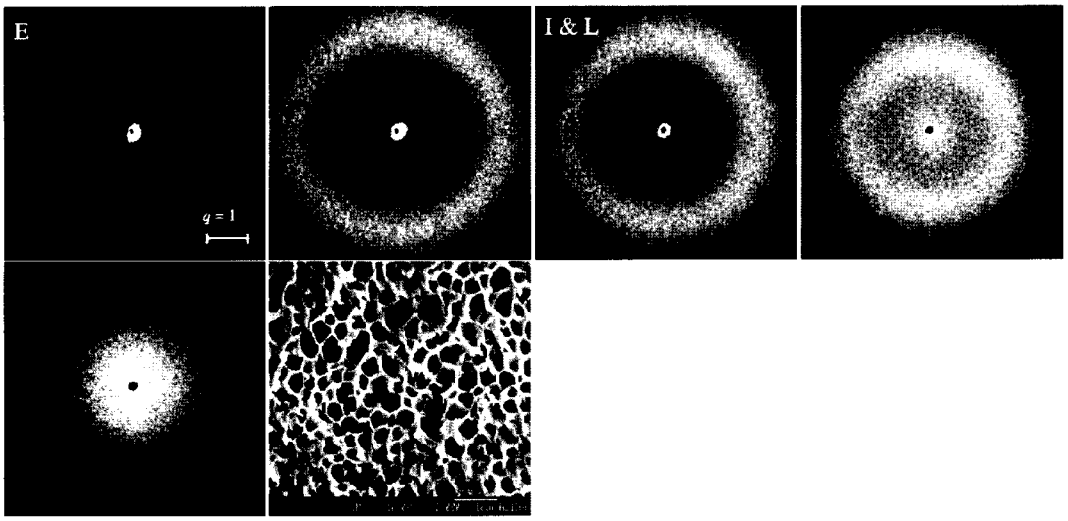

Fig. 8. The scattered light pattern progressed as a function of time during SD for 20Psf/70NMP/ 10n-butanol (w/w%).

observed.

It was observed from Figs. 5~8 that as the number of carbon of primary alcohol increased, q_m increased (compare the radii of rings presented in Figs 5~8). The interphase periodic distance between polymer rich-phases (Λ) decreased as the number of carbon of primary alcohol increased. These morphologies could be related to the position of the maximum scattering intensity ($\Lambda=2\pi/q_m$). As the scattering maximum occurred at the larger angles (larger q) in the order of n-butanol > n-propanol > methanol > no alcohol, the pore size of final morphology decreased. It was nearly impossible to determine quantitatively a relation between the domain size predicted by light scattering and measured in final structure, because of experimental limitation. However, as shown in FE-SEM, the

comparison of the light scattering prediction of phase separation with FE-SEM measurement showed the almost consistent tendency within reasonable limit.

Consequently, It was concluded from the experiment of SALS that the addition of different alcohol to dope solution brought about the different evolution of concentration fluctuation during phase separation, so that the distinctive light scattering patterns were followed.

4. Conclusions

We have shown the combined results of the scattering patterns with time evolution and the morphology by FE-SEM to investigate the effects of alcohol on two phases domain growth of PSf/NMP/alcohol solution and CPVC/THF/alcohol during water vapor induced phase separation, respectively. A typical scattering pattern of NG was observed for all casting solutions of CPVC/THF/alcohol: while the intensities continually decreased without displaying maximum I value, as q values increased, the intensity of the scattered light increased steadily with time. A typical scattering pattern of NG was observed for all casting solutions of CPVC/THF/alcohol: while the intensities continually decreased without displaying maximum I value, as q values increased, the intensity of the scattered light increased steadily with time. Meanwhile, in the case of PSf dope solution, the characteristic scattering patterns progressed by phase separation of SD was clearly observed. From the observation of the scattering patterns of PSf dope solution, as the scattering maximum occurred at the larger angles (larger q) in the order of n-butanol > n-propanol > methanol > no alcohol, the pore size of final morphology decreased. This result was quantitatively analyzed through the comparison of domain sizes from FE-SEM with size scales obtained from by SALS.

Acknowledgement

Jong Seok Kang is grateful to Brain Korea 21 for a scholarship. This work is supported by the Korea Institute of Science and Technology Evaluation and Planning (KISTEP) under the National Research Laboratory Program in the year 2002.

References and Notes

1. M. Mulder, "Basic Principles of Membrane Technology;" Kluwer Academic Publishers: Dordrecht, p 74 (1996).
2. P. van de Witte, P.J. Dijkstra, J.W.A. van der Berg, and J. Feijen, "Phase separation processes in polymer solutions in relation to membrane formation," *J. Membr. Sci.* **117**, 1 (1996).
3. S. Komura and H. Fukukawa, "Dynamics of ordering processes in condensed matter," NY: Plenum Press (1983).
4. J. D. Gunton, M. San Miguel, P. S. Sahni In: C. Domb, J. L. Lebowitz, "Phase transition and critical phenomena," Vol. 8, YN, Academic Press, (1983).
5. T. Hashimoto, "Self-assembly of polymer blends at phase separation morphology control by pinning of domain growth," In *Progress in Pacific Polymer Science*; Y. Imanish, Ed.; Springer: Berlin, Vol. 2, pp 175-187 (1992).
6. E. Schuhmacher, V. Soldi, and A. T. N. Pires, "PMMA or PEO in THF.H_2O mixture: phase diagram separation mechanism and application," *J. Membr. Sci.* **184**, 187 (2001).
7. H. Matsuyama, M. Teramoto, R. Nakatani, and T. Maki, "Membrane formation via phase separation induced by penetration of nonsolvent from vapor phase, II. Membrane morphology," *J. Appl. Polym. Sci.* vol. 74, 171 (1999).
8. K. V. Peinemann, J. F. Maggioni, and S. P. Nunes, "Poly(ether imide) membranes obtained from solution in cosolvent mixtures," *Polymer* **39**, 3411 (1998).
9. H. Matsutyama, M. Nishiguchi, and Y. Kitamura, "Phase separation mechanism during membrane formation by dry-cast process," *J. Appl. Polym. Sci.* **77**, 776 (2000).
10. R. Viswanathan and D. W. M. Marr, "AFM and SALS characterization of spherulitic structure in polyethylene," *Langmuir*, **12**, 1084 (1996)
11. S. P. Nunes and T. Inoue, "Evidence for

spinodal decomposition and nucleation and growth mechanisms during membrane formation," *J. Membr. Sci.* **111**, 93 (1996).
12. J. Szydlowski and A. van Hook, "Studies of liquid-liquid demixing of polystyrenes solutions using dynamic light scattering, nucleation and droplet growth from dilute solution," *Macromolecules* **31**, 3255 (1998).
13. T. Hashimoto, "Current topics in polymer science," Hanser, Munich, pp. 199 (1987).
14. J. G. Wijmans, H. J. J. Rutten, and C. A. Smolders, "Phase separation phenomena in solutions of poly((2,6-dimethyl-1.4-phenylene oxide) in mixtures of trichloroethylene, 1-octanol and methanol: relationship to membrane formation," *J. Polym. Sci., Polym. Phys. Ed.*, **23**, 1941 (1985).
15. P. D. Graham, A. J. Pervan, and A. J. McHugh, "The dynamics of thermal-induced phase separation in PMMA solutions," *Macromolecules* **30**, 1651 (1997).
16. J. W. Cahn, and J. E. Hilliard, "Free energy of a nonuniform system. I. Interfacial free energy," *J. Chem. Phy.*, **42**, 93 (1965).
17. J. Maugey, T. van Nuland, and P. Navard, "Small angle light scattering investigation of polymerization induced phase separation mechanisms," *Polymer* **42**, 4353 (2001).
18. K. Liu and E. Kiran, "Pressure-induced phase separation in polymer solutions: Kinetics of phase separation and crossover from nucleation and growth to spinodal decomposition in solutions of polyethylene in *n*-Pentane," *Macromolecules*, **34**, 3060-3068 (2001).